Physics of Fluids

RESEARCH ARTICLE | SEPTEMBER 13 2022

Viscoelastic and thixotropic characterization of paraffin/photopolymer composites for extrusion-based printing

Ciera E. Cipriani ; Yalan Shu (舒亚篮); Emily B. Pentzer ; Chandler C. Benjamin

Physics of Fluids 34, 093106 (2022)
https://doi.org/10.1063/5.0104157

Physics of Fluids ARTICLE scitation.org/journal/phf

Viscoelastic and thixotropic characterization of paraffin/photopolymer composites for extrusion-based printing

Cite as: Phys. Fluids **34**, 093106 (2022); doi: 10.1063/5.0104157
Submitted: 18 June 2022 · Accepted: 10 August 2022 ·
Published Online: 13 September 2022

Ciera E. Cipriani,[1] Yalan Shu (舒亚篮),[2] Emily B. Pentzer,[1,3] and Chandler C. Benjamin[2,a)]

AFFILIATIONS

[1]Department of Materials Science and Engineering, Texas A&M University, College Station, Texas 77845, USA
[2]Department of Mechanical Engineering, Texas A&M University, College Station, Texas 77843, USA
[3]Department of Chemistry, Texas A&M University, College Station, Texas 77843, USA

[a)]Author to whom correspondence should be addressed: ccbenjamin@tamu.edu

ABSTRACT

Three-dimensional printing (3DP) of functional materials is increasingly important for advanced applications requiring objects with complex or custom geometries or prints with gradients or zones with different properties. A common 3DP technique is direct ink writing (DIW), in which printable inks are comprised of a fluid matrix filled with solid particles, the latter of which can serve a dual purpose of rheology modifiers to enable extrusion and functional fillers for performance-related properties. Although the relationship between filler loading and viscosity has been described for many polymeric systems, a thorough description of the rheological properties of three-dimensional (3D) printable composites is needed to expedite the creation of new materials. In this manuscript, the relationship between filler loading and printability is studied using model paraffin/photopolymer composite inks containing between 0 and 73 vol. % paraffin microbeads. The liquid photopolymer resin is a Newtonian fluid, and incorporating paraffin microbeads increases the ink viscosity and imparts shear-thinning behavior, viscoelasticity, and thixotropy, as established by parallel plate rheometry experiments. Using Einstein and Batchelor's work on colloidal suspension rheology, models were developed to describe the thixotropic behavior of inks, having good agreement with experimental results. Each of these properties contributes to the printability of highly filled ($\geq$43 vol. % paraffin) paraffin/photopolymer composite inks. Through this work, the ability to quantify the ideal rheological properties of a DIW ink and to selectively control and predict its rheological performance will facilitate the development of 3D printed materials with tunable functionalities, thus, advancing 3DP technology beyond current capabilities.

Published by AIP Publishing. https://doi.org/10.1063/5.0104157

I. INTRODUCTION

Three-dimensional printing (3DP) is a manufacturing technique, which involves building up a three-dimensional (3D) object from a feedstock material. 3DP of functional materials is an increasingly important field with recent publications demonstrating applications spanning from printed sensors[1] to thermal energy storage devices[2] to biomedical devices,[3,4] to name a few. 3DP is preferable when objects with complex or custom geometries are desired. Furthermore, 3DP offers the ability to tune material composition on the fly, facilitating rapid prototyping by enabling variations in material chemistry,[5] changes to the type and loading level of fillers,[2,6] and combinations of multiple materials,[7] for example. Within advanced applications, the ability to 3D print lighter and more flexible polymeric structures with desired functionality is an emerging area of research. The extrusion-based 3DP process of direct ink writing (DIW) excels in this realm.[8] Feedstocks for DIW are viscous "inks," which are extruded through a nozzle in a predetermined pattern to build up printed objects. Thixotropy is required for DIW inks, so that they are shear thinning to be extruded, then quickly thicken to hold their shape until they are cured, or solidified, by one of a variety of methods, including liquid evaporation,[4] solvent removal,[1] and heat-[9] or light-induced[2,6,10] polymerization. Solid filler particles can impart such thixotropic behavior to Newtonian liquids.[1,2,11,12] Examples include clay,[11] silica,[11] salt,[12] or phase change material particles.[2]

Particle fillers can also facilitate the introduction of porosity into 3D printed structures, making them useful in applications requiring low mass, flexibility, and customizability. Sacrificial filler particles can be introduced into a matrix material to produce DIW inks, which are

printed, and the particles can be removed in post printing/processing steps. In these cases, the filler particles serve a dual purpose; not only do they facilitate the production of porous structures but also they adjust the viscosity of the 3DP ink. For example, Chen and coauthors[11] used clay and silica nanoparticles as sacrificial fillers in a solution of thermoplastic polyurethane to produce 3D printable inks. After printing and curing, the clay and silica were etched out using hydrofluoric acid, leaving pores within the structure, which were less than 5 μm in diameter. In a similar manner, Mu and coauthors[12] combined sodium chloride particles with photopolymer resins to make them 3D printable, then printed, and cured before removing the salt by soaking printed objects in water. Porous polymeric structures were prepared with pore sizes of 55–100, 200–250, or 350–450 μm, as determined by the size of the particles used. The Pentzer group[6] has previously reported paraffin/photopolymer composite inks, which can also be treated in this manner, where the 3D printed and cured photopolymer is a porous matrix and the solid paraffin is removed through solvent extraction. In this previous study, the relationships among particle loading, rheological performance, porosity, and mechanical properties of the 3D printed porous materials were described. The concentration of particle additives has been demonstrated to influence the viscosity and shear-thinning behavior of a 3DP ink,[1,2] along with the porosity of the resulting 3D printed porous object.[6,11,12] Thus, a more complete understanding of the rheological behavior of such materials is necessary to develop 3DP inks with desired printability and functionality, along with 3D printed porous objects with desired mechanical performance.

The relationship between filler particle loading and viscosity has been described for many polymeric systems, including liquid polymers,[1,13–15] melts,[16,17] and polymer solutions.[1,18–21] In this paper, we have used a phase change material filler to impart thixotropic behavior to a Newtonian photocurable resin to enable DIW of composites having varying loading levels of filler. The particles of the organic phase change material (PCM) paraffin wax were previously used to produce paraffin/photopolymer composite inks for DIW.[2,6] The particles imparted thioxotropy and also thermal energy regulation properties. Here, the photopolymer resin surrounds micrometer-scale particles of paraffin wax, the ink is printed by DIW, and the resin is cured with UV light. Thus, upon heating above the melting point of the PCM, the molten paraffin is contained within a cross-linked polymer matrix, and the overall structure is maintained over multiple heating-cooling cycles. Furthermore, the paraffin particles impart controllable thixotropic behavior to the Newtonian photopolymer resin, which facilitates DIW of these materials.[2] This enables the production of custom objects with passive thermal energy regulation capabilities such as components for decoration, restoration, or retrofitting of buildings. The paraffin/photopolymer composite inks can be modified for use with other PCMs to achieve different operation temperatures. A wide range of organic PCMs, which are most commonly paraffin waxes (C_nH_{2n+2}) and their fatty acid and ester derivatives,[22–28] can be readily incorporated into the photopolymer resin system. Our method of producing thermally regulating DIW inks allows for a modular approach to achieve desired PCM and matrix properties. A thorough description of the rheological properties of 3D printable composite inks will facilitate the development of materials with tunable functionalities, thereby enabling the application of 3DP technology in new arenas.

To describe the rheological properties of particle-filled DIW inks, such inks can be treated as colloidal suspensions.[29] One of the most striking features of colloidal suspensions is thixotropy, which is defined as the time dependent decrease in viscosity when shear flow is applied to a material previously at rest, and the subsequent recovery of viscosity when the flow is discontinued.[30–34] In the 1970s, Batchelor[35–37] derived the micromechanical theory for the rheology of colloidal suspension mechanics, often referred to as micromechanics. From Batchelor's research, it was discovered that the microstructure had to be taken into account when studying the mechanics of colloidal suspensions. The microstructure of a colloidal suspension and the evolution of the bulk properties of a material are coupled; thus, one does not change independent of the other. From this work, much of the foundation of colloidal sciences and modern colloidal suspension rheology was laid. For colloidal suspensions, it is noted that viscosity changes are a direct consequence of the interplay between hydrodynamic and Brownian forces.[34,36,37] When flow is applied to a colloidal fluid, anisotropy is introduced into its microstructure.[38,39] This anisotropy is a leading cause of the normal stress differences that are observed in these materials.[39] One common example of a thixotropic material is toothpaste, which flows when a shear stress is applied by extrusion from a tube and holds firm after extrusion onto a toothbrush. The DIW process requires thixotropic inks, which also exhibit this behavior.[8,29] Herein, we establish a relationship between the printability of paraffin/photopolymer resin composite inks and their rheological properties with a focus on viscoelasticity and thixotropy. By establishing this relationship, the interplay between rheology and 3D printability is better understood.[40] This work brings 3DP closer to informed customization of materials and better describes the intersection between printability and functionality.

II. METHODS

A. Materials

Elastic 50A photocurable resin designed for stereolithography 3DP was purchased from Formlabs (product # RS-F2-ELCL-01). Paraffin wax (CAS # 8002-74-2) and Span® 20 (CAS # 1338-39-2) were purchased from Sigma-Aldrich. Jacquard Piñata alcohol ink in the color sangria (# 015) was purchased from Amazon.

B. Instrumentation

Emulsification was performed using a Huxi JRJ300-SH high shear emulsifier. The inks were mixed in a Thinky AR-100 planetary mixer. 3D printing was performed on a Hyrel 3D Engine SR with an SDS-10 syringe extrusion head and a 365 nm UV Pen attachment. All shear rheometry experiments were conducted using an Anton Paar modular compact rheometer 302. A 25 mm parallel plate attachment was used with a 1 mm gap. Optical images of inks and printed objects were recorded using an iPhone 11 Pro.

C. Sample preparation

Span® 20 (0.5 ml) was dissolved in water (800 ml), and paraffin wax pellets (50 g) were added. The resulting mixture was heated to 80 °C to melt the wax. A high-shear emulsifier set at 6000 rpm for 3 min was used to form a wax-in-water emulsion. This emulsion was quenched in an ice water bath. Solid, spherical wax beads were collected by gravity filtration and washed with methanol. The wax beads, which were previously determined to have a mean diameter of 26 μm,[6] were dried under vacuum at room temperature overnight.

In a 20 ml scintillation vial wrapped with aluminum foil, dry wax beads were added to Formlabs elastic resin. Composite inks were produced containing 0, 10, 20,…, 60, 70 wt. % paraffin. Based on the densities of paraffin and Elastic resin (0.904 and 1.027 g/cm^3, respectively),[6] these composites contained 0, 11, 22, 33, 43, 53, 63, and 73 vol. % paraffin. Two batches of each ink were prepared to evaluate interbatch variability. Each mixture was thoroughly homogenized by mixing in a Thinky AR-100 planetary mixer in mixing mode for four 30 s intervals.

D. 3D Printing

3DP was performed in ambient conditions. Each ink containing 43 through 73 vol. % paraffin was loaded into a 10 ml syringe with an 18 gauge nozzle for 3DP. The loaded syringes were then placed on the extrusion cartridge of the 3D printer. Objects were printed onto a glass bed with a fixed layer height of 0.4 mm, an extrusion rate of 20 ml/h, and an infill of 30%. A 3D model of the Texas A&M mascot, Reveille, which was designed by user anberman, was downloaded from MakerBot Thingiverse. This model was printed using 63 vol. % paraffin ink and the above print settings. The model was exposed to ultraviolet light *in situ* for approximately 30 s after each layer was printed. Model inlays were printed with 63 vol. % paraffin ink mixed with Jacquard alcohol ink in the color sangria to produce a maroon color. After printing and UV curing, the substrate and inlays were assembled to create the final printed model.

E. Experimental procedure

All rheological testing was performed at 25 °C. To determine the limit of the linear viscoelastic region (LVER), or yield point of the inks, strain amplitude sweeps were conducted from 0.001% to 100% strain at a frequency of 1 s^{-1}. Three samples from two batches of each ink were measured for a total of six samples per ink. The yield point was defined as the strain amplitude at which the storage modulus differed from its maximum measured value by 5%. To evaluate the Newtonian and non-Newtonian behavior of these inks, the viscosity of each ink was measured over shear rates from 1 to 1000 s^{-1}. To determine whether the inks exhibited Newtonian, thixotropic, viscoelastic, or combination behavior, samples were subjected to a constant shear rate of 50 s^{-1} for 10 s, after which the shear rate was reduced to 0.1 s^{-1}, and the relaxation of the samples was monitored for 150 s.

F. Modeling of suspension rheometry

From the seminal work of Einstein[41] and Batchelor,[37] the viscosity of colloidal suspensions can be described in terms of the volume fraction ϕ of the dispersed particulates,

$$\eta(\phi) = \eta_m(1 + \alpha_1\phi + \alpha_2\phi^2 + \text{H.O.T.}), \tag{1}$$

where η_m is the viscosity of the suspending medium, α_1 and α_2 are known constants, which can vary slightly depending on the concentration of dispersed particulates, and H.O.T. represents higher order terms, which are generally small in magnitude. The value of α_1 is 2.5, and for dilute suspensions, the value of α_2 is 6.0. Based on Eq. (1), the viscosity change is strictly due to the volume fraction of paraffin, and additionally, the volume fraction does not change with time. The presence of the paraffin particles imparts thixotropic behavior, whereby the inks exhibit a time dependent change in viscosity with a change in the strain rate. Since the volume fraction of particles within an ink does not change, the thixotropic behavior is solely a result of the suspending medium. To model this thixotropic behavior, which is time dependent, we propose a model analogous to the model proposed by Bautista *et al.*[42] where, for the constitutive equation in our model, we use the convected Maxwell fluid model

$$\mathbf{T} = -p\mathbf{I} + \mathbf{S}, \quad \mathbf{S} + \lambda_m \overset{o}{\mathbf{S}} = 2\eta\mathbf{D}, \tag{2}$$

where $\mathbf{T}$ is the Cauchy stress, $\mathbf{S}$ is the extra stress, sometimes referred to as the viscous stress, λ_m is the structure-related characteristic time, and the corotational derivative is given as

$$\overset{o}{\mathbf{S}} = \frac{D\mathbf{S}}{Dt} + \mathbf{S}\mathbf{W} - \mathbf{W}\mathbf{S}. \tag{3}$$

The material derivative, D/Dt, and the rate of strain tensor, $\mathbf{D}$, are defined by

$$\begin{aligned} \frac{D\mathbf{S}}{Dt} &= \frac{\partial \mathbf{S}}{\partial t} + \text{grad}\,\mathbf{S}\cdot\mathbf{v}, \\ \mathbf{L} &\equiv \text{grad}\,\mathbf{v} = \mathbf{D} + \mathbf{W}, \\ \mathbf{D} = \frac{1}{2}(\mathbf{L} + \mathbf{L}^{\mathrm{T}}), &\quad \mathbf{W} = \frac{1}{2}(\mathbf{L} - \mathbf{L}^{\mathrm{T}}), \quad \mathbf{L} = \dot{\boldsymbol{\gamma}}, \end{aligned} \tag{4}$$

where $\mathbf{L}$ is the velocity gradient, $\mathbf{v}$ is the velocity, $\mathbf{D}$ is the rate of the strain tensor, and $\mathbf{W}$ is the vorticity tensor, which are the symmetric and antisymmetric parts of the velocity gradient. For the experiments conducted herein, we apply a sinusoidal strain and strain rate as follows:

$$\boldsymbol{\gamma} = \gamma_o \sin(\omega t)\,\mathbf{e}_{\boldsymbol{\theta}} \otimes \mathbf{e}_{\mathbf{z}}, \quad \dot{\boldsymbol{\gamma}} = \gamma_o\omega\cos(\omega t)\,\mathbf{e}_{\boldsymbol{\theta}} \otimes \mathbf{e}_{\mathbf{z}}, \tag{5}$$

and for the stress vs strain rate experiments, we have

$$\boldsymbol{\gamma} = \gamma_o\,\mathbf{e}_{\boldsymbol{\theta}} \otimes \mathbf{e}_{\mathbf{z}}, \quad \dot{\boldsymbol{\gamma}} = \dot{\gamma}_o\,\mathbf{e}_{\boldsymbol{\theta}} \otimes \mathbf{e}_{\mathbf{z}}. \tag{6}$$

To model the thixotropic behavior, we will consider the following evolution equation for the viscosity proposed by Fredrickson:[34]

$$\frac{\partial\psi}{\partial t} = \frac{\psi_o - \psi}{\lambda} + k(\psi_\infty - \psi)\mathbf{T} : \mathbf{D}, \tag{7}$$

where k is the kinetic constant that governs the breakdown of the structure of the suspension, whereas λ is the structure relaxation time of the suspending medium, a structural buildup time. ψ_o is the fluidity at low shear rate, ψ_∞ is the fluidity at high shear rate, and $\mathbf{T} : \mathbf{D}$ is the stress power. Fredrickson's evolution equation is written in terms of the fluidity, ($\psi = \eta^{-1}$). The convected Maxwell constituitive equation is usually coupled with Fredrickson's evolution Eq. (7) to account for thixotropic behavior.

For simple shear flow, in the first interval, the sample is sheared at a constant and steady shear rate. At some points, the flow is suddenly stopped, or the shear rate is reduced to a very low value. For the case of simple shear flow, Eqs. (7) and (2) can be written as a scalar equation,

$$\frac{\partial\psi}{\partial t} = \frac{\psi_o - \psi}{\lambda} + k(\psi_\infty - \psi)\tau_{12}\dot{\gamma}. \tag{8}$$

In this type of experiment, the sample is sheared at a constant shear rate for the first 10 s and then the shear rate is suddenly dropped to a much smaller value, which we can regard it as zero. Hence, we set $\dot{\gamma}$ in Eq. (8) as zero, and after integration

$$\psi = \psi_0 + (\psi_\infty - \psi_0)\exp\left[-t/\lambda\right]. \tag{9}$$

Writing the equation in the form of viscosity as

$$\eta_m = \frac{\eta_0\eta_\infty}{\eta_\infty + (\eta_0 - \eta_\infty)\exp\left[-t/\lambda\right]}. \tag{10}$$

The slight modification to the viscosity arises from the fact that Eq. (10) only governs the viscosity of the suspending medium. This assumption is based on Eq. (1), in which the total viscosity is simply the viscosity of the matrix material multiplied by a function of the volume fraction of the particulate material. Based on this analysis, we propose the following equations:

$$\begin{aligned} \eta_s(t,\phi) &= f(t)g(\phi), \\ f(t) &= \underbrace{\frac{\eta_0\eta_\infty}{\eta_\infty + (\eta_0 - \eta_\infty)\exp\left[-t/\lambda\right]}}_{\text{thixotropic}}, \\ g(\phi) &= \underbrace{(1 + \alpha_1\phi + \alpha_2\phi^2)}_{\text{phase volume}}, \end{aligned} \tag{11}$$

where $f(t)$ describes the time dependent thixotropic contribution to the viscosity of the suspending medium η_m[42] and $g(\phi)$ describes the contribution of the volume fraction of solid particles.

Equation (11) was used to describe the behavior of composites containing different volume fractions of paraffin microbeads when subjected to a constant shear rate of 50 s^{-1} for 10 s, which was then reduced to 0.1 s^{-1} for 150 s. Since the effects of thixotropic behavior are displayed immediately after the change in the shear rate, the first 20 s after the drop of shear rate were used to develop the model. The curve_fit function in Python, which uses a least squares method for curve fitting, was used to determine the structural buildup time λ, along with parameters η_o, η_∞, and the coefficient of determination R^2 for each paraffin/photopolymer composite.

III. RESULTS AND DISCUSSION

The level of paraffin loading in the photopolymer resin greatly influences the rheological performance of the inks. As demonstrated by the digital image of the inks in Fig. 1(a), the pure photopolymer resin is a viscous liquid, which forms a puddle when deposited onto a surface. Increasing paraffin loading visibly increases the viscosity of the inks and the ability for the inks to hold their shape when deposited onto a surface. Inks containing between 43 and 73 vol. % paraffin are 3D printable by DIW.[2,6] Inks contain < 43 vol. % paraffin pool and do not hold their shape when extruded, whereas inks containing higher loadings of paraffin (i.e., up to 73 vol. %) are able to be extruded and maintain the shape of printed objects, so long as the inks contain enough resin to envelop the paraffin particles. For example, the letters T, A, M, and U were 3D printed using inks containing 43, 53, 63, and 73 vol. % paraffin, respectively [Fig. 1(b)]. Variations in rheological performance are observed in these digital images. The 43 vol. % paraffin ink behaved in a more fluid-like manner with the ink being readily extruded from an 18 gauge nozzle and the extruded filaments merging with one another. With increasing paraffin loading, the extrusion of the ink from the nozzle was qualitatively observed to require more force. The quality of the extruded filaments improved with increased paraffin loading with discrete yet well-joined filaments being most obvious in the ink containing 63 vol. % paraffin (the letter M). The ink containing 73 vol. % paraffin was difficult to extrude from an 18 gauge nozzle, which resulted in some irregularities, such as gaps between printed filaments, as seen in the letter U. Fidelity can be improved by increasing the nozzle size to accommodate the increased viscosity of more highly filled samples, and similarly, by decreasing the nozzle size to print the 43 vol. % paraffin ink. The paraffin/photopolymer composite inks are printable, and the rheological performance of a DIW ink can be modified to enable printing with a certain nozzle size to achieve a desired resolution. To demonstrate the printing of more detailed objects, a 3D model of the Texas A&M mascot, Reveille, was printed using the 63 vol. % paraffin ink [Fig. 1(c)]. The inlays were

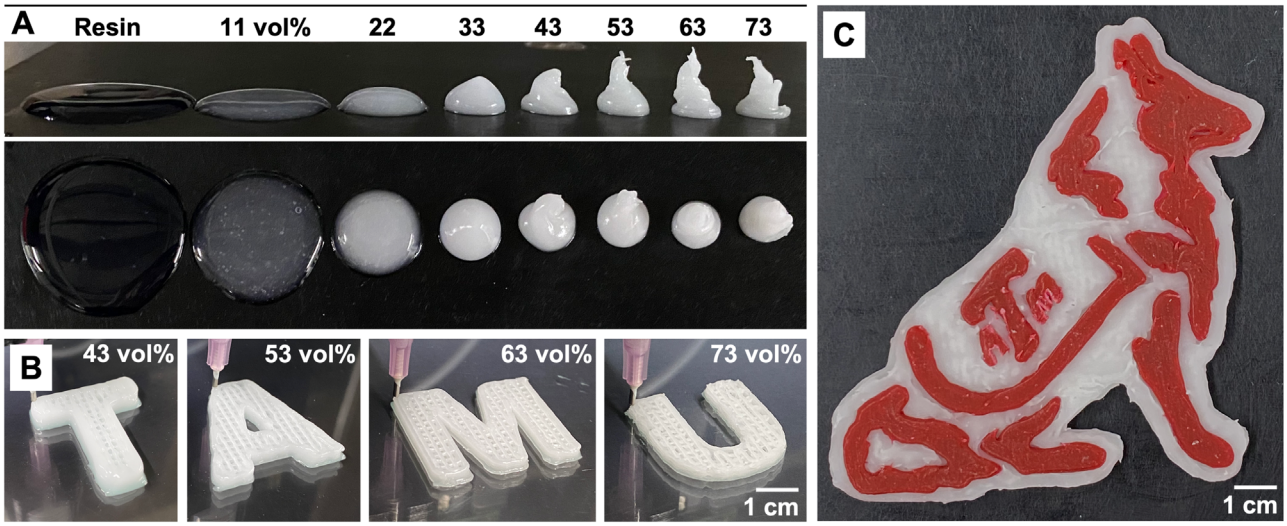

FIG. 1. (a) Digital image of paraffin/photopolymer composite inks containing between 0 and 73 vol. % paraffin microbeads. (b) Digital images of printable paraffin/photopolymer composite inks containing between 43 and 73 vol. % paraffin being printed by DIW. (c) Model of Reveille 3D printed using the ink containing 63 vol. % paraffin.

printed using the ink mixed with a Jacquard alcohol ink dye in the color sangria. This model was printed in parts with the main outline, and the inlays separate from one another. After printing and curing with UV light, the maroon inlays were inserted into the white substrate. These paraffin/photopolymer composite inks can readily accommodate the printing of objects with complex geometries.

The results from strain amplitude sweeps on three representative inks are displayed in Fig. 2(a), and the results for the two batches of each composite, as well as overall averages for all composites, are provided in Fig. S1. These oscillatory tests were performed at a frequency of 1 s^{-1}. There were not notable differences between different batches of the same composite. The limit of the linear viscoelastic region (LVER), or the yield point, was determined by identifying the strain amplitude at which the storage modulus differed from its initial value by 5%. Yielding is a continuum, rather than instantaneous, transition.[43] Therefore, there are several methods for determining the apparent yield point, which give slightly different numerical results. These methods include extrapolating the onset of yielding from the plateau and linear shear-thinning portions of the plotted data or specifying a fraction of the initial value of G′ as a threshold below which yielding is said to have occurred.[44] In the present work, the latter method was used. Specifically, the reduction in G′ to 95% of its initial plateau value indicates the start of breakdown of the ink structure, at which flow should begin,[45] and extrusion from a DIW syringe nozzle should be possible. Notably, G′ and G″ are known to depend on oscillation frequency;[46] as such, the results reported here apply to the case of oscillation at a frequency of 1 s^{-1}. The corresponding strain amplitude and modulus values for all inks are plotted in Fig. 2(b), and numerical results are provided in Table S1.

As shown in Fig. 2(a), for photopolymer resin containing no paraffin filler, the loss modulus had no dependence on strain amplitude and maintained a constant value of approximately 22 Pa throughout the strain amplitude sweep. The resin storage modulus was nearly zero throughout the strain amplitude sweep. This is attributed to viscous behavior dominating the response of the liquid photopolymer resin, as indicated by the greater value of the loss modulus compared to the storage modulus at all strain amplitudes. The incorporation of paraffin microbeads into the photopolymer resin resulted in a marked change in flow properties during the strain amplitude sweep. Specifically, increased paraffin loading resulted in increased values of G′ and G″ and decreased strain amplitude at the yielding point. The higher G′ values indicate that, as expected, the incorporation of filler particles increased the elastic behavior of the material. Additionally, increased particle loading results in a higher degree of interparticle friction, hence the higher values of G″.[47]

Both the storage and loss moduli decreased with increasing strain amplitude for all particle-containing inks with this effect becoming more exaggerated as the filler content increased. This expected behavior is highlighted in Fig. 2(b), where a higher volume fraction of paraffin beads caused deviations from constant modulus values to occur at lower strain amplitudes. The extent of the LVER of a filled composite depends on the loading of the filler. Previous reports on highly filled polymeric fluids have found that the strain amplitude at which a composite deviates from linearity decreases as the volume fraction of filler increases.[48] These results may arise from the increased presence of particle aggregates in more highly filled samples. Such particle aggregates are termed "flocs," because they are comprised of multiple particles that have flocculated together with each floc effectively acting as a single large particle unless it is broken down by shear stress.[49] In general, more highly filled samples exhibit a higher propensity for floc formation as a result of van der Waals interactions between particles. The breakdown or partial breakdown of these flocs into discrete particles could contribute to the decreased strain amplitude at yield, or LVER limit, as paraffin loading was increased. In the future, such relationships can be tied to various printing parameters, such as nozzle size, flow rate, print speed, and temperature, to predict a range of filler/matrix compositions that may be printable by DIW.

To elucidate non-Newtonian characteristics of the paraffin/photopolymer composite inks, the shear rate was modulated in one of two ways—continuously or in a stepwise manner. For the former case, a shear rate sweep was performed on each ink, the shear stress was measured, and viscosity was calculated [Figs. 3(a) and S2]. The photopolymer

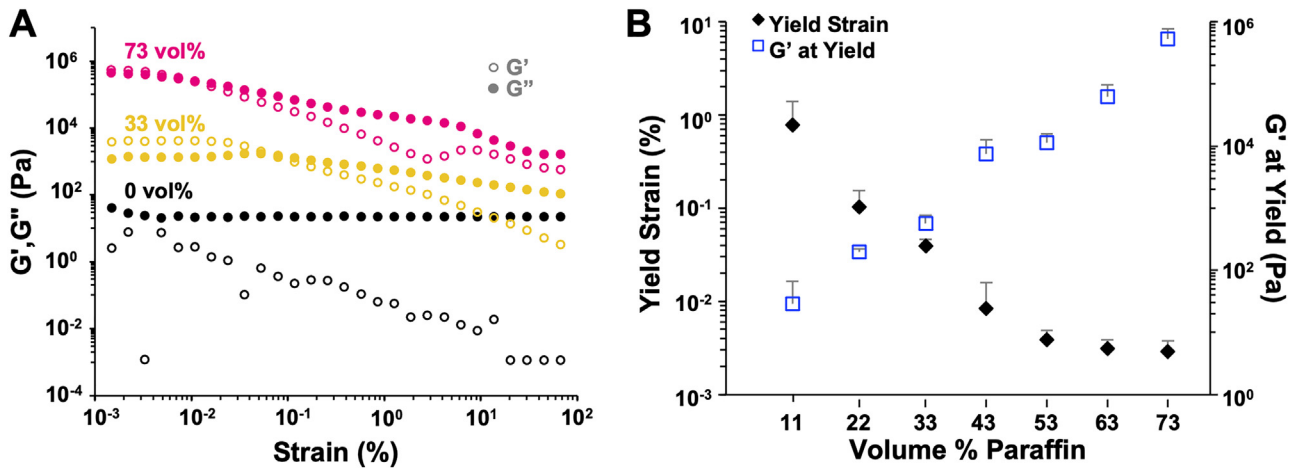

FIG. 2. (a) Average storage and loss moduli during the strain amplitude sweep from 0.001% to 100% strain for photopolymer resin (i.e., 0 vol. % paraffin), 33 vol. %, and 73 vol. % paraffin composite inks (oscillation frequency of 1 s^{-1}). (b) Plot of the average storage modulus at yield and average yield strain for all composite inks, measured at the crossover point of G′ and G″. Error bars indicate standard deviation (n = 6).

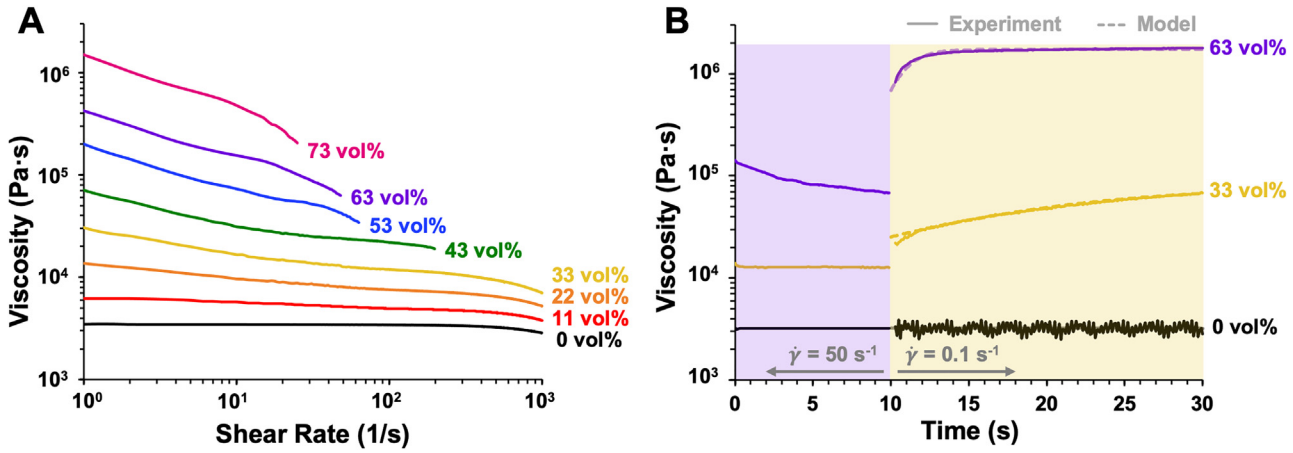

FIG. 3. (a) Average (n = 6) viscosity of resin and inks as the shear rate was increased from 1 to 1000 s^{-1}. (b) Average experimental (n = 6) and modeled viscosity response of resin, 33 vol. % paraffin, and 63 vol. % paraffin inks for the first 30 s of the shear rate drop experiment. During the first 10 s of test time (shaded in purple), samples were subjected to a shear rate of 50 s^{-1}, then the shear rate was dropped to 0.1 s^{-1} (shaded in yellow).

resin displayed Newtonian behavior with a viscosity independent of shear rate. For the paraffin-filled inks, the viscosity decreased with increasing shear rate, which indicates shear-thinning behavior. The magnitude of the shear-thinning behavior increases with increasing paraffin loading. Notably, inks containing ≥ 43 vol. % paraffin were expelled from the sides of the parallel plates at high shear rates, and therefore, the data are truncated at those points of expulsion. The full data plotted in Fig. S2 indicate low interbatch variability. Thus, incorporating paraffin microbeads into the Newtonian photopolymer resin imparts non-Newtonian, shear-thinning behavior, which is consistent across composite batches. The magnitude of shear thinning increases with increased paraffin loading, thus enabling DIW printing of highly filled inks (73 vol. % paraffin).

Alongside high viscosity and shear-thinning behavior, thixotropy is an integral property of inks for DIW. Thixotropy is a result of the reversible local spatial rearrangement of components within a material (in the present case, the rearrangement of paraffin microbeads within the photopolymer resin).[49] This rearrangement is time-dependent; therefore, the structure buildup constant λ is integral to describe the thixotropy of these particle-filled composites. The tendency of a sample to expel from the sides of a parallel plate attachment is commonly observed in thixotropic materials.[50] We sought to determine the extent of thixotropy for these 3D printable inks.[51] Extrusion of an ink from a 3D printer can be modeled where the application of force during extrusion is treated as a high shear rate step, and the cessation of flow upon deposition of the ink is treated as a low shear rate step. Therefore, each ink was subjected to a shear rate of 50 s^{-1} for 10 s, then allowed to relax at 0.1 s^{-1} for 150 s. A plot of average viscosity over time for the resin, 33 vol. % paraffin, and 63 vol. % paraffin inks for the first 30 s of the shear rate drop experiment is displayed in Fig. 3(b). Full experimental data for both batches of each ink are available in Fig. S3, and full modeled data are plotted against the experimental data for each ink in Fig. S4.

The thixotropic behavior of the paraffin/photopolymer composite inks can be attributed to microscale phenomena. As previously discussed, it is believed that interparticle interactions, specifically van der Waals forces, produce flocs in filled composites. Flocs can break down under high stress then build up once the stress is relieved.[49,50] Resin was expected to possess time-independent behavior, as it did not contain paraffin microbeads, and therefore, no floc formation should occur. This behavior is evident from the data in Fig. 3(b), as the resin maintained a consistent viscosity value in both steps of the experiment. Adding paraffin microbeads to the resin caused the composite viscosity to increase notably after the step decrease in shear rate. The magnitude of this viscosity increase was directly related to the level of paraffin loading and, thus, can be correlated with floc formation. The plots in Fig. S3 also indicate that more highly filled composites reached stable viscosity values within a shorter time after the reduction in shear rate. Furthermore, there was negligible difference between results for different batches of the same ink, except for batch 2 of the ink containing 11 vol. % paraffin. The effects of interbatch variability are magnified when paraffin loading is low, because each individual floc has a larger impact on the sample behavior than more highly filled samples with a higher number of flocs. Therefore, slight differences in floc formation between the two batches could have had a marked effect on the measured results. Furthermore, the less filled samples possess smaller viscosity values. Therefore, small differences between measured viscosities are larger in relation to measured values for these samples as compared to more highly filled samples, whereas small differences between batches of more highly filled samples would not be as noticeable in the final data. For DIW inks, the shear rate-dependence of viscosity is of utmost importance, as an ink should be extrudable at the force and shear rate applied by the printer, and then the ink viscosity should quickly increase so that the printed object holds its shape, and more ink can be extruded atop it.

We sought to model the thixotropic behavior of these inks by fitting Eq. (11) to the experimental data. This model, deduced from the upper convected Maxwell constitutive equation and a kinematic equation, has an exponential form which matches our experimental data well. Model parameters are provided in Table I. The value of λ was determined for six datasets (three samples from batch 1 and three from batch 2). The coefficient of determination (R^2) values for λ for

TABLE I. Structure buildup time constant for Eq. (11) for each paraffin/photopolymer composite ink after the step change in the shear rate.

Vol. % paraffin	λ (s)	R^2 for λ	R^2 for model
0	445	0.569	0.794
11	44.5	0.904	0.894
22	41.1	0.926	0.978
33	23.7	0.962	0.987
43	15.1	0.924	0.973
53	11.2	0.972	0.968
63	3.77	0.918	0.854
73	77.5	0.781	0.838

each composite are provided in the second column, and the R^2 values comparing the model results and experimental results are provided in the third column. Resin, having 0 vol. % paraffin, shows no thixotropic behavior, since no flocs form or break down with the step change of shear rate. Therefore, the structure buildup time constant λ is abnormally large, and the R^2 values for resin are small. As for the ink containing 73 vol. % paraffin, we hypothesize that the high loading of paraffin caused slip to occur between the ink and the parallel plates of the rheometer, resulting in a large value of λ. This wall slip phenomenon has been previously demonstrated for colloidal suspensions when subjected to large deformation,[52–55] particularly those having high filler loading levels, which cause them to possess solid-like behavior which contributes to slip.[54] Excluding the extreme scenarios of resin and ink containing 73 vol. % paraffin, a trend is observed: λ decreases with increasing loading of paraffin microbeads. This is because an ink having a higher volume percent of microbeads displays a quicker response toward the shear rate change, and a stable condition is achieved more quickly. Additionally, the higher the loading of paraffin microbeads, the larger the final stable viscosity will be, as indicated in Fig. 3(b).

IV. CONCLUSIONS

In summary, we have reported the viscoelastic and thixotropic performance of paraffin/photopolymer composites, which can be harnessed as 3D printable inks for the facile process of direct ink writing. Paraffin microbeads were leveraged as rheology modifiers to impart increased viscosity, shear-thinning behavior, viscoelasticity, and thixotropy to a Newtonian photopolymer resin. Each of these properties contributes to the printability of highly filled paraffin/photopolymer composite inks (i.e., containing $\geq$ 43 vol. % paraffin). This printability was demonstrated by extrusion of the inks from various sized nozzles and the subsequent ability of highly filled inks to retain shape after extrusion. Having established printability, strain amplitude sweeps were performed on the inks to determine the influence of paraffin loading on the limit of the linear viscoelastic range, i.e., the yield point. It was found that photopolymer resin exhibited a response characteristic of a viscous fluid, whereas particle-filled inks had viscoelastic responses in which the storage and loss moduli intersected to indicate flow. The yield point occurred at lower strains as paraffin loading increased, and this phenomenon was attributed to the breakdown of more flocs of paraffin particles in more highly filled inks. Alongside viscoelastic characteristics, the shear-thinning behavior of the inks was examined via shear rate sweeps. Photopolymer resin displayed Newtonian behavior, whereas the incorporation of paraffin imparted shear-thinning behavior, with the magnitude increasing with increased paraffin loading. Therefore, the yield point and viscosity of a filled composite can be controlled by the filler loading level to facilitate printing by DIW. The printability of a DIW ink depends on both the viscosity and the magnitude of the thixotropic response, which are both tunable by the filler loading level. To simulate extrusion from a DIW printer, each composite was subjected to a step reduction in shear rate, and the material viscosity was monitored over time. This experiment was modeled using Eq. (11), which was derived from the upper convected Maxwell constitutive equation and a kinetic equation. The regression result indicates that the structure buildup time constant λ decreases as the volume percent of paraffin in the ink increases. It was determined that photopolymer resin alone does not exhibit any shear-dependent behavior, but incorporating paraffin microbeads produces a thixotropic response which can be described well by our constitutive equations. Increasing paraffin loading was found to decrease the time required for a given ink to achieve a stable viscosity value after the reduction in shear rate. Yielding behavior, viscosity, and viscoelasticity are useful quantities for predicting the printability of a material by DIW.

Looking forward, the ability to describe the ideal rheological properties of a DIW ink and to selectively control its rheological performance will facilitate the development of 3D printed materials with tunable functionalities. A deeper understanding of the requirements for DIW inks is an urgent need, which can be met by mathematical descriptions of rheological behavior. In the future, inks may be screened for printability based on parameters for shear-thinning and thixotropic performance to develop a predictive model. Matrix-filler interactions are key to ink printability, so variations in matrix rheology and particle morphology could be described to improve printability predictions. This model would eliminate the guess-and-check approach of current DIW ink formulations, which would enable the use of new materials in 3DP and bring DIW technology to its full potential.

SUPPLEMENTARY MATERIAL

See the supplementary material for the average storage and loss moduli during the strain amplitude sweep from 0.001% to 100% strain for both batches of all samples, numerical values of yield strain and modulus for the composites, average viscosity as shear rate was increased from 1 to 1000 s^{-1} for both batches of all samples, average viscosity of both batches of all samples as shear rate was dropped from 50 to 0.1 s^{-1}, and the plot of experimental and modeled viscosities immediately after shear rate drop.

ACKNOWLEDGMENTS

The authors acknowledge Dr. Peiran Wei for developing the paraffin/photopolymer composite inks and for providing the 3D model of the letters T, A, M, and U. Jordan Price is acknowledged for assisting with 3D printing. The authors thank Dr. Manoj Myneni, Dr. Parvin Karimineghlani, and Alexandra Treviño for consultation on rheological testing, alongside Abdelrahman Youssef for consultation on modeling the thixotropic behavior of the inks. C.E.C. is supported by a NASA Space Technology Graduate

Research Opportunity. E.B.P. acknowledges NSF DMR via No. 2103182.

AUTHOR DECLARATIONS

Conflict of Interest

The authors have no conflicts to disclose.

Author Contributions

Ciera E Cipriani: Data curation (equal); Formal analysis (equal); Validation (equal); Writing – original draft (equal); Writing – review & editing (equal). **Yalan Shu:** Data curation (equal); Formal analysis (equal); Validation (equal); Writing – original draft (equal); Writing – review & editing (equal). **Emily Pentzer:** Project administration (equal); Supervision (equal); Writing – review & editing (equal). **Chandler Benjamin:** Conceptualization (lead); Project administration (equal); Supervision (equal); Writing – review & editing (equal).

DATA AVAILABILITY

The data that support the findings of this study are available within the article and its supplementary material.

REFERENCES

[1]P. Wei, H. Leng, Q. Chen, R. C. Advincula, and E. B. Pentzer, "Reprocessable 3D-printed conductive elastomeric composite foams for strain and gas sensing," ACS Appl. Polym. Mater. **1**, 885–892 (2019).
[2]P. Wei, C. E. Cipriani, and E. B. Pentzer, "Thermal energy regulation with 3D printed polymer-phase change material composites," Matter **4**, 1975–1989 (2021).
[3]J. Lai, X. Ye, J. Liu, C. Wang, J. Li, X. Wang, M. Ma, and M. Wang, "4D printing of highly printable and shape morphing hydrogels composed of alginate and methylcellulose," Mater. Des. **205**, 109699 (2021).
[4]B. Zhang, S. H. Chung, S. Barker, D. Craig, R. J. Narayan, and J. Huang, "Direct ink writing of polycaprolactone/polyethylene oxide based 3D constructs," Prog. Nat. Sci. **31**, 180–191 (2021).
[5]M. M. Durban, J. M. Lenhardt, A. S. Wu, W. Small IV, T. M. Bryson, L. Perez-Perez, D. T. Nguyen, S. Gammon, J. E. Smay, E. B. Duoss, J. P. Lewicki, and T. S. Wilson, "Custom 3D printable silicones with tunable stiffness," Macromol. Rapid Commun. **39**, 1700563 (2018).
[6]C. E. Cipriani, T. Ha, O. B. Martinez Defilló, M. Myneni, Y. Wang, C. C. Benjamin, J. Wang, E. B. Pentzer, and P. Wei, "Structure–processing–property relationships of 3D printed porous polymeric materials," ACS Mater. Au **1**, 69–80 (2021).
[7]C. Yuan, F. Wang, B. Qi, Z. Ding, D. W. Rosen, and Q. Ge, "3D printing of multi-material composites with tunable shape memory behavior," Mater. Des. **193**, 108785 (2020).
[8]J. A. Lewis, "Direct ink writing of 3D functional materials," Adv. Funct. Mater. **16**, 2193–2204 (2006).
[9]I. D. Robertson, M. Yourdkhani, P. J. Centellas, J. E. Aw, D. G. Ivanoff, E. Goli, E. M. Lloyd, L. M. Dean, N. R. Sottos, P. H. Geubelle *et al.*, "Rapid energy-efficient manufacturing of polymers and composites via frontal polymerization," Nature **557**, 223–227 (2018).
[10]C. B. Arrington, D. A. Rau, C. B. Williams, and T. E. Long, "Uv-assisted direct ink write printing of fully aromatic Poly(amide imide)s: Elucidating the influence of an acrylic scaffold," Polymers **212**, 123306 (2021).
[11]Q. Chen, P.-F. Cao, and R. C. Advincula, "Mechanically robust, ultraelastic hierarchical foam with tunable properties via 3D printing," Adv. Funct. Mater. **28**, 1800631 (2018).
[12]X. Mu, T. Bertron, C. Dunn, H. Qiao, J. Wu, Z. Zhao, C. Saldana, and H. Qi, "Porous polymeric materials by 3D printing of photocurable resin," Mater. Horiz. **4**, 442–449 (2017).
[13]T. Kaully, A. Siegmann, and D. Shacham, "Rheology of highly filled natural $CaCO_3$ composites. II. Effects of solid loading and particle size distribution on rotational rheometry," Polym. Compos. **28**, 524–533 (2007).
[14]J. Chong, E. Christiansen, and A. Baer, "Rheology of concentrated suspensions," J. Appl. Polym. Sci. **15**, 2007–2021 (1971).
[15]A. Poslinski, M. Ryan, R. Gupta, S. Seshadri, and F. Frechette, "Rheological behavior of filled polymeric systems II. The effect of a bimodal size distribution of particulates," J. Rheol. **32**, 751–771 (1988).
[16]T. Honek, B. Hausnerova, and P. Saha, "Relative viscosity models and their application to capillary flow data of highly filled hard-metal carbide powder compounds," Polym. Compos. **26**, 29–36 (2005).
[17]A. Mayadunne, S. Bhattacharya, and E. Kosior, "Modelling of packing behavior of irregularly shaped particles dispersed in a polymer matrix," Powder Technol. **89**, 115–127 (1996).
[18]T. Matsumoto, C. Hitomi, and S. Onogi, "Rheological properties of disperse systems of spherical particles in polystyrene solution at long time-scales," Trans. Soc. Rheol. **19**, 541–555 (1975).
[19]M. A. Haney, "The differential viscometer. I. A new approach to the measurement of specific viscosities of polymer solutions," J. Appl. Polym. Sci. **30**, 3023–3036 (1985).
[20]D. W. Sundstrom, "Viscosity of suspensions in polymeric solutions," Rheol. Acta **22**, 420–423 (1983).
[21]T. Stephens, H. Winter, and M. Gottlieb, "The steady shear viscosity of filled polymeric liquids described by a linear superposition of two relaxation mechanisms," Rheol. Acta **27**, 263–272 (1988).
[22]A. Arshad, M. Jabbal, Y. Yan, and J. Darkwa, "The micro-/nano-PCMs for thermal energy storage systems: A state of art review," Int. J. Energy Res. **43**, 5572–5620 (2019).
[23]D. Zhou, C.-Y. Zhao, and Y. Tian, "Review on thermal energy storage with phase change materials (PCMs) in building applications," Appl. Energy **92**, 593–605 (2012).
[24]D. Hawes, D. Feldman, and D. Banu, "Latent heat storage in building materials," Energy Build. **20**, 77–86 (1993).
[25]F. Kuznik, D. David, K. Johannes, and J.-J. Roux, "A review on phase change materials integrated in building walls," Renewable Sustainable Energy Rev. **15**, 379–391 (2011).
[26]S. A. Memon, "Phase change materials integrated in building walls: A state of the art review," Renewable Sustainable Energy Rev. **31**, 870–906 (2014).
[27]H. Akeiber, P. Nejat, M. Z. A. Majid, M. A. Wahid, F. Jomehzadeh, I. Z. Famileh, J. K. Calautit, B. R. Hughes, and S. A. Zaki, "A review on phase change material (PCM) for sustainable passive cooling in building envelopes," Renewable Sustainable Energy Rev. **60**, 1470–1497 (2016).
[28]E. Shchukina, M. Graham, Z. Zheng, and D. Shchukin, "Nanoencapsulation of phase change materials for advanced thermal energy storage systems," Chem. Soc. Rev. **47**, 4156–4175 (2018).
[29]S. Tagliaferri, A. Panagiotopoulos, and C. Mattevi, "Direct ink writing of energy materials," Mater. Adv. **2**, 540–563 (2021).
[30]T. Peterfi, "Die abhebung der befruchtungsmembran bei seeigeleiern: Eine kolloidchemische Analyse des Befruchtungsvorganges," Wilhelm Roux'Arch. Entwickl. Org. **112**, 660–695 (1927).
[31]C. J. Dimitriou and G. H. McKinley, "A comprehensive constitutive law for waxy crude oil: A thixotropic yield stress fluid," Soft Matter **10**, 6619–6644 (2014).
[32]M. Agarwal, S. Sharma, V. Shankar, and Y. M. Joshi, "Distinguishing thixotropy from viscoelasticity," J. Rheol. **65**, 663–680 (2021).
[33]R. Larson, "Constitutive equations for thixotropic fluids," J. Rheol. **59**, 595–611 (2015).
[34]A. Fredrickson, "A model for the thixotropy of suspensions," AIChe J. **16**, 436–441 (1970).
[35]G. Batchelor, "The stress system in a suspension of force-free particles," J. Fluid Mech. **41**, 545–570 (1970).
[36]G. Batchelor, "Brownian diffusion of particles with hydrodynamic interaction," J. Fluid Mech. **74**, 1–29 (1976).
[37]G. Batchelor, "The effect of brownian motion on the bulk stress in a suspension of spherical particles," J. Fluid Mech. **83**, 97–117 (1977).
[38]N. Martys, M. Khalil, W. George, D. Lootens, and P. Hébraud, "Stress propagation in a concentrated colloidal suspension under shear," Eur. Phys. J. E **35**, 1–7 (2012).

[39]L. E. Sánchez-Diáz, T. Iwashita, T. Egami, and W.-R. Chen, "Connection between the anisotropic structure and nonlinear rheology of sheared colloidal suspensions investigated by Brownian dynamics simulations," J. Phys. Commun. **3**, 055018 (2019).
[40]M. Monteferrante, A. Montessori, S. Succi, D. Pisignano, and M. Lauricella, "Lattice boltzmann multicomponent model for direct-writing printing," Phys. Fluids **33**, 042103 (2021).
[41]A. Einstein, *Investigations on the Theory of the Brownian Movement* (Courier Corporation, 1956).
[42]F. Bautista, J. De Santos, J. Puig, and O. Manero, "Understanding thixotropic and antithixotropic behavior of viscoelastic micellar solutions and liquid crystalline dispersions. I. The model," J. Non-Newtonian Fluid Mech. **80**, 93–113 (1999).
[43]G. J. Donley, P. K. Singh, A. Shetty, and S. A. Rogers, "Elucidating the G″ overshoot in soft materials with a yield transition via a time-resolved experimental strain decomposition," Proc. Natl. Acad. Sci. U. S. A. **117**, 21945–21952 (2020).
[44]M. Dinkgreve, J. Paredes, M. M. Denn, and D. Bonn, "On different ways of measuring 'the' yield stress," J. Non-Newtonian Fluid Mech. **238**, 233–241 (2016).
[45]C. Christopoulou, G. Petekidis, B. Erwin, M. Cloitre, and D. Vlassopoulos, "Ageing and yield behaviour in model soft colloidal glasses," Philos. Trans. R. Soc. A **367**, 5051–5071 (2009).
[46]J.-F. Berret, "Rheology of wormlike micelles: Equilibrium properties and shear banding transitions," in *Molecular Gels: Materials with Self-Assembled Fibrillar Networks*, edited by R. G. Weiss and P. Terech (Springer Netherlands, Dordrecht, 2006), pp. 667–720.
[47]M. M. Rueda, M.-C. Auscher, R. Fulchiron, T. Perie, G. Martin, P. Sonntag, and P. Cassagnau, "Rheology and applications of highly filled polymers: A review of current understanding," Prog. Polym. Sci. **66**, 22–53 (2017).
[48]M. Bek, J. Gonzalez-Gutierrez, C. Kukla, K. Pušnik Črešnar, B. Maroh, and L. Slemenik Perše, "Rheological behaviour of highly filled materials for injection moulding and additive manufacturing: Effect of particle material and loading," Appl. Sci. **10**, 7993 (2020).
[49]H. A. Barnes, *A Handbook of Elementary Rheology* (University of Wales, 2000), Vol. 1.
[50]J. Mewis, "Thixotropy-a general review," J. Non-Newtonian Fluid Mech. **6**, 1–20 (1979).
[51]J. Choi, M. Armstrong, and S. A. Rogers, "The role of elasticity in thixotropy: Transient elastic stress during stepwise reduction in shear rate," Phys. Fluids **33**, 033112 (2021).
[52]A. Abbasi Moud, J. Poisson, Z. M. Hudson, and S. G. Hatzikiriakos, "Yield stress and wall slip of kaolinite networks," Phys. Fluids **33**, 053105 (2021).
[53]M. Cloitre, "Yielding, flow, and slip in microgel suspensions: From microstructure to macroscopic rheology," *Microgel Suspensions: Fundamentals and Applications*, edited by A. Fernandez-Nieves, H. Wyss, J. Mattsson, and D. A. Weitz (John Wiley & Sons, 2011), pp. 283–309.
[54]M. Cloitre and R. T. Bonnecaze, "A review on wall slip in high solid dispersions," Rheol. Acta **56**, 283–305 (2017).
[55]B. L. Walter, J.-P. Pelteret, J. Kaschta, D. W. Schubert, and P. Steinmann, "On the wall slip phenomenon of elastomers in oscillatory shear measurements using parallel-plate rotational rheometry: I. Detecting wall slip," Polym. Testing **61**, 430–440 (2017).